Neuropsychiatric Disease and Treatment

Dovepress

open access to scientific and medical research

Open Access Full Text Article

ORIGINAL RESEARCH

Comparison of spontaneous brain activity revealed by regional homogeneity in AQP4-IgG neuromyelitis optica-optic neuritis versus MOG-IgG optic neuritis patients: a resting-state functional MRI study

This article was published in the following Dove Press journal:
Neuropsychiatric Disease and Treatment
24 October 2017
Number of times this article has been viewed

Junqing Wang[1,*]
Yuan Tian[2,*]
Yi Shao[3,*]
Hui Feng[1]
Limin Qin[1]
Weiwei Xu[1]
Hongjuan Liu[1]
Quangang Xu[1]
Shihui Wei[1]
Lin Ma[2]

[1]Department of Ophthalmology, [2]Department of Radiology, Chinese PLA General Hospital, Beijing, [3]Department of Ophthalmology, the First Affiliated Hospital of Nanchang University, Nanchang, Jiangxi, People's Republic of China

*These authors contributed equally to this work

Correspondence: Shihui Wei
Department of Ophthalmology, Chinese PLA General Hospital, Fuxing Road No 28, Haidian District, Beijing 100853, People's Republic of China
Tel +86 10 6693 8375
Email weishihui706@hotmail.com

Lin Ma
Department of Radiology, Chinese PLA General Hospital, Fuxing Road No 28, Haidian District, Beijing, People's Republic of China
Tel +86 138 0122 2069
Email cjr.malin@vip.163.com

Objective: Many previous studies have demonstrated that neuromyelitis optica (NMO) patients have abnormalities of brain anatomy and function. However, differences in spontaneous brain activity between myelin oligodendrocyte glycoprotein (MOG)-IgG ON and aquaporin 4(AQP4)-neuromyelitis optica-optic neuritis (ON) remain unknown. In the current study, we investigated the brain neural homogeneity in MOG-IgG ON versus AQP4-IgG NMO-ON subjects by regional homogeneity (ReHo) method using magnetic resonance imaging (MRI).

Patients and methods: A total of 32 NMO-ON and ON subjects (21 with AQP4-IgG+NMO-ON and 11 with MOG-IgG+ON) and 34 healthy controls (HCs) closely matched for age were recruited, and scans were performed for all subjects. A one-way analysis of variance (ANOVA) was performed to determine the regions in which the ReHo was different across the three groups. NMO-ON and ON subjects were distinguished from HCs by a receiver operating characteristic (ROC) curve. The relationship between the mean ReHo in many brain regions and clinical features in NMO subjects was calculated by Pearson correlation analysis.

Results: Compared with HCs, MOG-IgG+ON subjects had significantly decreased ReHo values in the posterior lobe of the left cerebellum and increased ReHo values in the left inferior frontal gyrus, right prefrontal gyrus, and left precentral/postcentral gyrus. AQP4-IgG+NMO-ON subjects showed higher ReHo values in the left inferior frontal gyrus and right middle temporal/occipital gyrus. Compared with MOG-IgG+ON subjects, AQP4-IgG+NMO-ON subjects had lower ReHo values in the posterior lobe of the right cerebellum.AQP4-Ig+NMO-ON subjects showed higher ReHo values in the left precentral/postcentral gyrus and right superior temporal gyrus.

Conclusion: AQP4-IgG+NMO-ON and MOG-IgG+ON subjects showed abnormal synchronized neuronal activity in many brain regions, which is consistent with deficits in visual, motor, and cognitive function. Furthermore, different patterns of synchronized neuronal activity occurred in the AQP4-IgG+NMO-ON and MOG-IgG+ON.

Keywords: neuromyelitis optica-optic neuritis, MOG-IgG, AQP4-IgG, regional homogeneity, resting state, functional magnetic resonance imaging

Introduction

Neuromyelitis optica (NMO) is an inflammatory demyelinating disorder. The prevalence of NMO ranges from 0.51/100,000 in Cuba to 4.4/100,000 in Southern Denmark.[1] NMO leads to spinal cord lesions,[2] as well as optic nerve impairments,[3]

and is characterized by the presence of aquaporin-4 (AQP4)-IgG+[4] or myelin oligodendrocyte glycoprotein (MOG)-IgG+ autoantibodies.[5] Compared with MOG-IgG+NMO, AQP4-IgG+NMO presents more frequently with optic neuritis (ON) and transverse myelitis.[6] The MOG-IgG+NMO showed more retinal nerve fiber layer may be preserved than AQP4-IgG+NMO.[7] Currently, corticosteroids and plasma exchange are effective treatment of acute NMO patients.[8,9] Besides, immunosuppressive drugs such as mycophenolate mofetil and azathioprine have been shown to be effective in NMO disorders.[10] A recent study demonstrated that rituximab therapy reduces the frequency of NMO relapses and neurological disability in NMO patients.[11]

Functional magnetic resonance imaging (fMRI) and diffusion tensor imaging (DTI) are used to evaluate pathological changes of the brain in NMO disorders. A previous study demonstrated that compared with AQP4+ disease, AQP4– NMO patients have a higher incidence of brain lesions and infratentorial lesions.[12] Meanwhile, the AQP4 antibody-related disease and MOG antibody NMO were shown to be associated with different brain lesions.[13] Liu et al[14] found that NMO was associated with spinal cord atrophy and mild brain atrophy. However, NMO patients with cognitive impairment show atrophy in the deep gray matter (GM).[15] Rivero et al[16] demonstrated that NMO was accompanied by decreased fractional anisotropy (FA) values and increased mean diffusivity (MD) values in MRI images of the lesion sites in the cervical spinal cord using the DTI method. Moreover, NMO spectrum disorders showed that GM and white matter (WM) atrophy was correlated with retinal nerve fiber layers.[17] NMO was also associated with abnormal structural and functional connectivity in the visual cortex.[18] However, the abovementioned studies focused on anatomic abnormalities of the brain and spinal cord in NMO patients. Our understanding of spontaneous brain activity in NMO patients remains very limited.

Synchronized neuronal activity occurs in the normal human brain.[19] Previous studies have indicated that synchronized neuronal activity plays a critical role in neural information processing.[20–22] The regional homogeneity (ReHo) method, using resting-state fMRI (rs-fMRI) measurements, is believed to be a reliable and sensitive way to evaluate the coherence of the blood-oxygen-level-dependent (BOLD) signal among neighboring voxels of the whole brain at rest.[23,24] Thus, the ReHo method can measure local synchronization of spontaneous fMRI signals and has been successfully applied to assess the spontaneous brain activity in many diseases such as major depressive disorder,[25] sleep disorders,[26] and Alzheimer's disease.[27] Moreover, Liang et al[28] found that NMO patients have significant ReHo decreases in multiple brain regions.

The aim of this study was to evaluate the abnormal synchronization of neuronal activity in AQP4-IgG+NMO-ON and MOG-IgG+ON patients. Furthermore, ReHo identified differences between the AQP4-IgG+NMO-ON and MOG-IgG+ON.

Materials and methods

Subjects

The research protocol was approved by the medical ethics committee and Department of Ophthalmology, Chinese PLA General Hospital. A total of 32 NMO-ON and ON patients (22 with AQP4-IgG+NMO-ON and 11 with MOG-IgG+ON) were recruited from the Department of Ophthalmology, Chinese PLA General Hospital. The inclusion criteria of the study in NMO[29] and ON were as follows: 1) extended visual evoked potential (VEP) P100 latency periods (bilateral or unilateral); 2) acute ON; 3) optic nerve MRI with T2 - weighted hyperintense lesion or T1-weighted gadolinium-enhancing lesion extending over >1/2 optic nerve length or involving optic chiasma; 4) positive serum AQP4-IgG or MOG-IgG. The exclusion criteria of the study in NMO and ON were as follows: 1) any evidence of compressive, ischemic, toxic, genetic, metabolic, or invasive optic neuropathy; 2) acute vision loss due to retinal disease, sympathetic ophthalmia, or nervous system disease; 3) obvious abnormality in brain parenchyma by brain MRI; 4) congenital or acquired diseases, such as psychiatric disorder, hypertension, diabetes mellitus, or coronary artery disease, and no addictions such as heroin, smoking, or alcohol; 5) receipt of organ transplant; 6) extremely under or over weight (body mass index is <18.5 or > 24.9 kg/m^2).

A total of 34 healthy controls (HCs; 18 males and 16 females) who were age status matched to subjects in the NMO-ON and ON groups were also recruited for this study. All HCs met the following criteria: 1) no ocular disease with uncorrected visual acuity (VA) > 1.0; 2) no psychiatric disorders (depression, bipolar disorder, or sleep disorders); and 3) able to be scanned with MRI (eg, not having a cardiac pacemaker or implanted metal devices).

The research methods in the study complied with the principles of the Declaration of Helsinki. All subjects were adults and informed of the purpose, methods, and potential risks entailed in the study before providing their written informed consent.

MRI parameters

MRI scanning was performed on a 3 T MR scanner (Trio; GE Healthcare Europe GmbH, Freiburg, Germany). The

whole-brain T1-weighted images were obtained with a spoiled gradient-recalled echo sequence with the following parameters: repetition time =1,900 ms, echo time =2.26 ms, thickness =1.0 mm, gap =0.5 mm, acquisition matrix =256 ×256, field of view =250×250 mm, and flip angle =9°. Functional images with the parameters, such as repetition time =2,000 ms, echo time =30 ms, thickness =4.0 mm, gap =1.2 mm, acquisition matrix =64×64, flip angle =90°, field of view =220×220 mm, 29 axial, were corrected.

fMRI data processing

The functional images were analyzed as described previously.[30] Briefly, the data were filtered by software (www.MRIcro.com) and preprocessed using Statistical Parametric Mapping SPM8 (http://www.fil.ion.ucl.ac.uk/spm/) and Data Processing Assistant for rs-fMRI DPARSFA (http://rfmri.org/DPARSF) software.[31] After head motion corrections and spatial smoothing, the fMRI images were de-trended and band pass filtered (0.01–0.08 Hz) to reduce the effects of low-frequency drift and physiological high-frequency respiratory and cardiac noise.[32] Based on Kendall's coefficient of concordance (KCC), each voxel in the brain was calculated voxel-wise by applying a cluster size of 26 voxels. ReHo computation was performed with REST (http://www.restfmri.net) software.[23] Individual ReHo maps were generated by calculating the KCC of the time series of a given voxel with those of its nearest neighbors (26 voxels) in a voxel-wise manner with the formula:

$$\mathrm{ReHo} = \frac{\sum (R_i)^2 - n(\bar{R})^2}{k^2(n^3 - n)/12}$$

where ReHo is the KCC for a given voxel, ranging from 0 to 1. When the ranked time series is more consistent with its adjacent ones, the KCC value is closer to 1; k is the voxel number among time series (in our study, k =27, including one given voxel that was located in the cubic center and its adjacent 26 voxels); n is the number of ranks; R_i is the sum rank of the ith time point, and $R = (n + 1)/2*k/2$ is the mean of the R_i's. The KCC value refers to the central voxel among the cluster. The individual KCC ReHo map was generated on a voxel-wise basis for all data sets. To reduce the influence of individual variations in the KCC value, normalization of ReHo maps was performed by dividing the KCC among each voxel by the averaged KCC of the whole brain. The resulting fMRI data were then spatially smoothed with a Gaussian kernel of 6×6×6 mm^3 full width at half maximum.

Statistical analysis

For the cumulative clinical measurements, chi-square test was used for gender and optic neuritis episode comparisons. Then, independent sample t-test was used for duration of NMO-ON or ON and time since last relapse comparisons. One-way analysis of variance (ANOVA) with Bonferroni post hoc test was used for age and Expanded Disability Status Scale (EDSS) comparisons using SPSS version 16.0 (SPSS Inc., Chicago, IL, USA).

A one-way ANOVA was used to identify regions in which the spontaneous activity pattern was different between the AQP4-IgG+NMO-ON and MOG-IgG+ON groups and HCs. We performed post hoc analysis tests after regressing out age and gender effects to compare the ReHo values between each pair of groups ($P<0.01$, cluster >40 voxels, and AlphaSim corrected).

The relationship between the mean ReHo value of NMO subjects and the clinical features was analyzed by a Pearson correlation analysis using SPSS version 16.0 ($P<0.05$ was considered to be a significant difference).

Results

Demographics and visual measurements

AQP4-IgG+NMO-ON and MOG-IgG+ON subjects showed significantly higher scores in EDSS ($P<0.001$) compared with HCs. Meanwhile, NMO-ON or ON subjects showed significant difference in best-corrected VA-oculus dexter (OD) ($P<0.001$) and best-corrected VA-oculus sinister (OS) ($P<0.001$) compared with HCs. There were no significant differences in the age, gender, optic neuritis episodes, time since last relapse, and durations between the groups (Table 1).

ReHo differences

A one-sample t-test was performed to extract the ReHo results across the subjects within each group ($P<0.05$). Intra-group comparisons within the AQP4-IgG+NMO-ON and MOG-IgG+ON and HCs groups are shown in Figure 1.

A one-way ANOVA was used to identify regions in which the spontaneous activity pattern was different across the three groups. Then, post hoc analysis tests were used to compare the ReHo values between each pair of groups.

AQP4-IgG+NMO-ON versus HCs

Compared with HCs, AQP4-IgG+NMO-ON subjects showed significantly decreased ReHo values in the left inferior frontal gyrus (IFG; Figure 2A and B [blue] and Table 2). AQP4-IgG+NMO-ON subjects showed increased ReHo values in the right middle temporal (MT)/occipital gyrus (Figure 2A and B [red] and Table 2) with $P<0.01$ for multiple comparisons using Gaussian random field (GRF) theory, ($z > 2.3$, $P<0.01$, cluster >40 voxels, and AlphaSim corrected). The mean values of altered ReHo between the two groups are shown in Figure 2C.

Table 1 Demographics and clinical measurements by groups

Condition	MOG-IgG+ON	AQP4-IgG+NMO-ON	HCs	*P*-values
Male/female	4/7	0/21	11/23	0.010
Age (years)	32.18±3.99	37±8.79	36.33±6.23	0.154
Handedness	11R	21R	34R	N/A
Duration (months)	31.18±16.05	35.09±13.40	N/A	0.469
Best-corrected VA-OD	0.64±0.57	0.62±0.54	1.11±0.18	<0.001
Best-corrected VA-OS	0.65±0.56	0.65±0.59	1.10±0.19	<0.001
Optic neuritis episodes (L/R)	6/5	11/10	N/A	0.907
Time since last relapse (days)	40.90±9.95	41.29±8.99	N/A	0.914
EDSS	4.77±1.08	4.90±1.22	0.78±0.51	<0.001
Current immunotherapy	Azathioprine	Azathioprine	N/A	N/A

Notes: Data presented as mean ± standard deviation, unless otherwise specified. Chi-square test was used for gender and optic neuritis episode comparisons. Independent sample *t*-test was used for duration of NMO-ON and ON and time since last relapse comparisons. One-way ANOVA with Bonferroni post hoc test was used for age and EDSS comparisons.

Abbreviations: ANOVA, analysis of variance; AQP4, aquaporin-4; EDSS, Expanded Disability Status Scale; HCs, healthy controls; MOG, myelin oligodendrocyte glycoprotein; N/A, not applicable; NMO, neuromyelitis optica; ON, optic neuritis; VA, visual acuity; OD, oculus dexter; OS, oculus sinister; R, right.

AQP4-IgG+NMO-ON versus MOG-IgG+ON

Compared with MOG-IgG+ON subjects, AQP4-IgG+NMO-ON subjects showed significantly decreased ReHo values in the left precentral/postcentral gyrus and right superior temporal gyrus (Figure 3A and B [blue] and Table 2); AQP4-IgG+NMO-ON subjects showed increased ReHo values in the right cerebellum posterior lobe (CPL; Figure 3A and B [red] and Table 2) with $P<0.01$ for multiple comparisons using GRF theory ($z>2.3$, $P<0.01$, cluster >40 voxels, AlphaSim corrected). The mean values of altered ReHo between the two groups are shown in Figure 3C.

MOG-IgG+ON versus HCs

Compared with HCs, the MOG-IgG+ON subjects showed significantly decreased ReHo values in the posterior lobe of the left cerebellum (Figure 4A and B [blue] and Table 2). MOG-IgG+ON subjects showed increased ReHo values in the left IFG, right prefrontal gyrus, and left precentral/postcentral gyrus (Figure 4A and B [red] and Table 2) with $P<0.01$ for multiple comparisons using GRF theory ($z>2.3$, $P<0.01$, cluster >40 voxels, AlphaSim corrected). The mean values of altered ReHo between the two groups are shown in Figure 4C.

Receiver operating characteristic (ROC) curve

We speculated that the ReHo differences between the two groups might be useful diagnostic markers. Thus, the ROC curve method was used to assess the mean ReHo values in the different brain regions. The areas under the ROC curve were as follows: 0.780 for the left IFG (AQP4-IgG+NMO-ON > HCs, Figure 5A); 0.795 for the right MT/occipital gyrus (AQP4-IgG+NMO-ON < HCs, Figure 5B); 0.835 for the right CPL (AQP4-IgG+NMO-ON > MOG-IgG+ON, Figure 5C); 0.803 for the left precentral/postcentral gyrus; 0.855 for the right superior temporal gyrus (AQP4-IgG+NMO-ON < MOG-IgG+ON, Figure 5D); 0.884 for the right CPL (MOG-IgG+ON < HCs, Figure 5E); 0.925 for the left IFG; 0.869 for the right prefrontal gyrus; and 0.872 for the left precentral/postcentral gyrus (MOG-IgG+ON > HCs, Figure 5F).

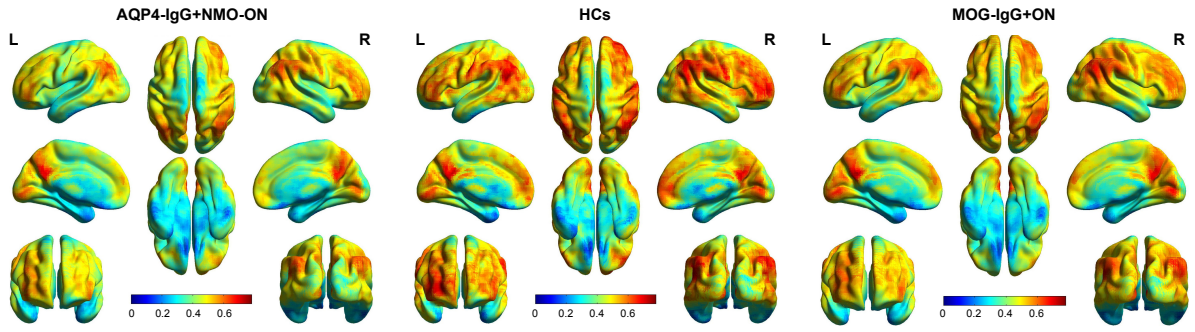

Figure 1 One-sample *t*-test results.

Note: Within-group ReHo maps within the AQP4-IgG+NMO-ON (left) and HCs (middle) and MOG-IgG+ONs (right; $P<0.001$, FDR corrected).

Abbreviations: AQP4, aquaporin-4; HCs, healthy controls; L, left; MOG, myelin oligodendrocyte glycoprotein; NMO, neuromyelitis optica; ON, optic neuritis; R, right; ReHo, regional homogeneity; FDR, false discovery rate.

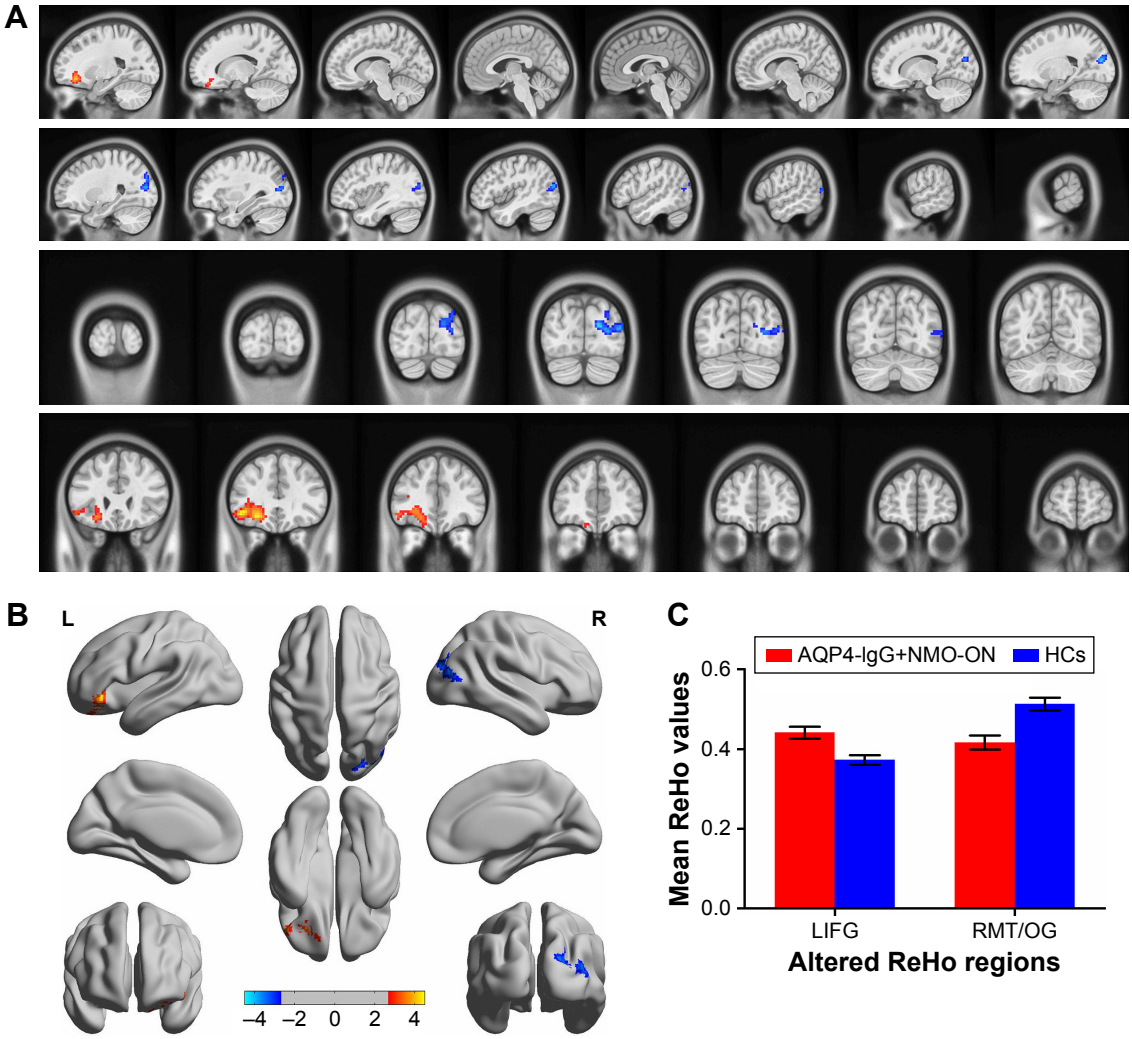

Figure 2 Spontaneous brain activity in the AQP4-IgG+NMO-ON and HCs groups.
Notes: Significant activity differences were observed in the LIFG and RMT/OG. The red or yellow denotes higher ReHo values, and the blue areas indicate lower ReHo values ($P<0.01$ for multiple comparisons using GRF theory ($z>2.3$, $P<0.01$, cluster >40 voxels, AlphaSim corrected) (**A** and **B**). The mean values of altered ReHo values between the AQP4-IgG+NMO-ON and HC groups (**C**).
Abbreviations: AQP4, aquaporin-4; GRF, Gaussian random field; HCs, healthy controls; L, left; LIFG, left inferior frontal gyrus; NMO, neuromyelitis optica; ON, optic neuritis; R, right; ReHo, regional homogeneity; RMT/OG, right middle temporal/occipital gyrus.

Table 2 Brain areas with significantly different ReHo values across three groups

Condition	Brain regions	Cluster size	MNI			T-values
			X (mm)	Y (mm)	Z (mm)	
AQP4-IgG+NMO-ON versus HCs						
AQP4 > HCs	Left IFG	272	−42	33	−6	4.514
AQP4 < HCs	Right MT/occipital gyrus	242	18	−84	21	−4.213
AQP4-IgG+NMO-ON versus MOG-IgG+ON						
AQP4 > MOG	Right CPL	352	24	−39	−57	4.037
AQP4 < MOG	Left precentral/postcentral gyrus	860	−54	−6	36	−4.942
AQP4 < MOG	Right superior temporal gyrus	670	48	−12	12	−5.077
MOG-IgG+ON versus HCs						
MOG < HCs	Left CPL	596	−51	−69	−45	−4.465
MOG > HCs	Left IFG	916	−30	15	3	5.583
MOG > HCs	Right prefrontal gyrus	649	27	21	0	4.556
MOG > HCs	Left precentral/postcentral gyrus	306	−57	−12	15	4.262

Note: The statistical threshold was set at the voxel level with $P<0.05$ for multiple comparisons using GRF theory ($z>2.3$, $P<0.01$, cluster >40 voxels, AlphaSim corrected).
Abbreviations: AQP4, aquaporin-4; CPL, cerebellum posterior lobe; GRF, Gaussian random field; HCs, healthy controls; IFG, inferior frontal gyrus; MNI, Montreal Neurological Institute; MOG, myelin oligodendrocyte glycoprotein; MT, middle temporal; NMO, neuromyelitis optica; ON, optic neuritis; ReHo, regional homogeneity.

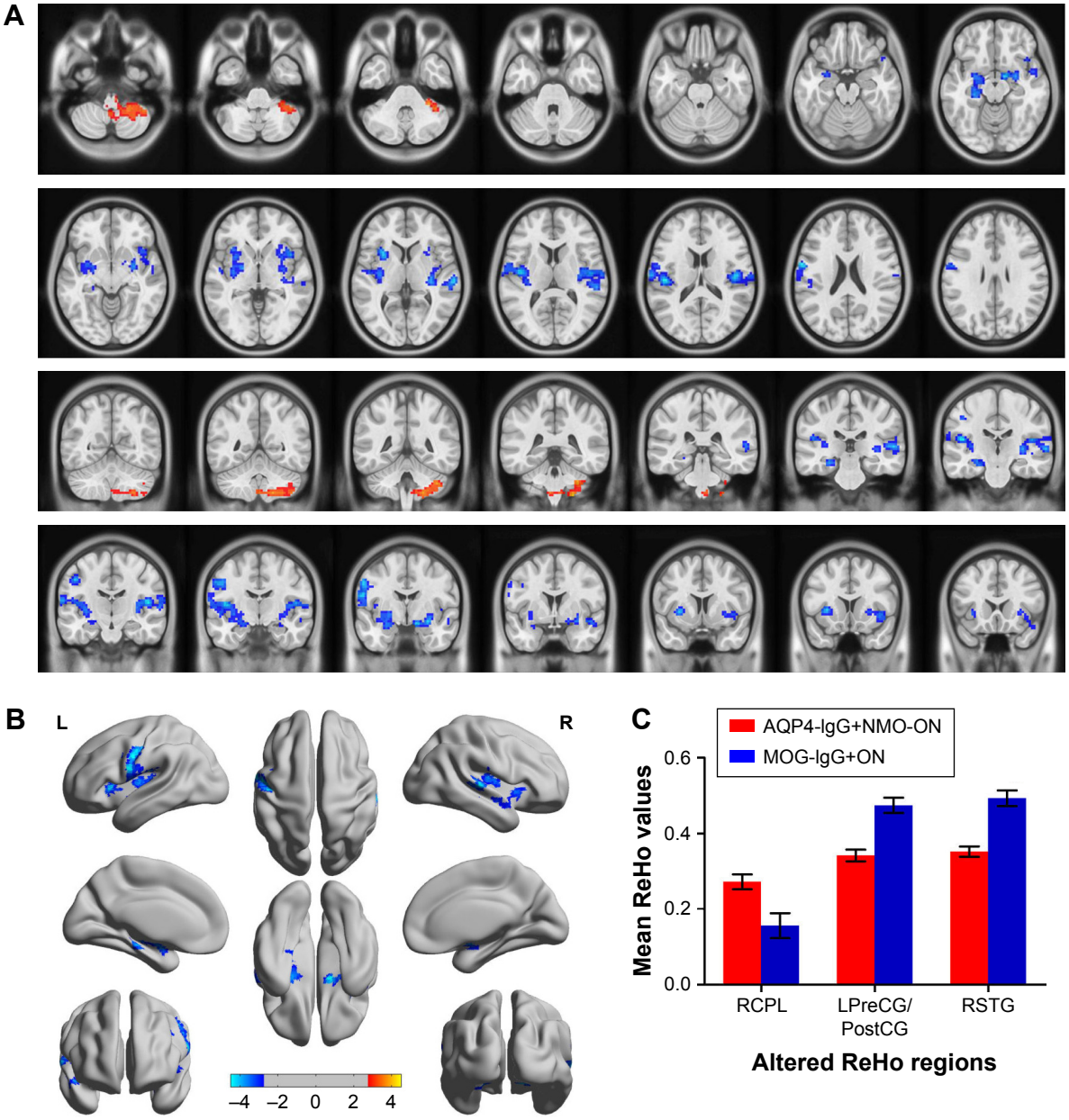

Figure 3 Spontaneous brain activity in the AQP4-IgG+NMO-ON and MOG-IgG+ON groups.
Notes: Significant activity differences were observed in the RCPL, LPreCG/PostCG, and RSTG. The red or yellow denotes higher ReHo values, and the blue areas indicate lower ReHo values ($P<0.01$ for multiple comparisons using GRF theory ($z>2.3$, $P<0.01$, cluster >40 voxels, AlphaSim corrected) (**A** and **B**). The mean values of altered ReHo values between the AQP4-IgG+NMO-ON and MOG-IgG+ON groups (**C**).
Abbreviations: AQP4, aquaporin-4; GRF, Gaussian random field; L, left; LPreCG/PostCG, left precentral/postcentral gyrus; MOG, myelin oligodendrocyte glycoprotein; NMO, neuromyelitis optica; ON, optic neuritis; R, right; RCPL, right cerebellum posterior lobe; ReHo, regional homogeneity; RSTG, right superior temporal gyrus.

Discussion

ReHo is an effective and noninvasive rs-fMRI technique to assess synchronized neuronal activity in the brain. Our study is the first to compare synchronized neuronal activity levels occurring in AQP4-IgG+NMO-ON and MOG-IgG+ON subjects. In the AQP4-IgG+NMO-ON group, lower ReHo values are present in the right MT/occipital gyrus, while higher ReHo values are found in the left IFG (compared with the HCs). In the MOG-IgG+ON group, lower ReHo values are found in the posterior lobe of the left cerebellum, while higher ReHo values occur in the left IFG, right prefrontal gyrus, and left precentral/postcentral gyrus compared with the HCs. Furthermore, the AQP4-IgG+NMO-ON group showed lower ReHo values in the left precentral/postcentral gyrus and right superior temporal gyrus and higher ReHo values in the posterior lobe of the right cerebellum compared with the MOG-IgG+ON group.

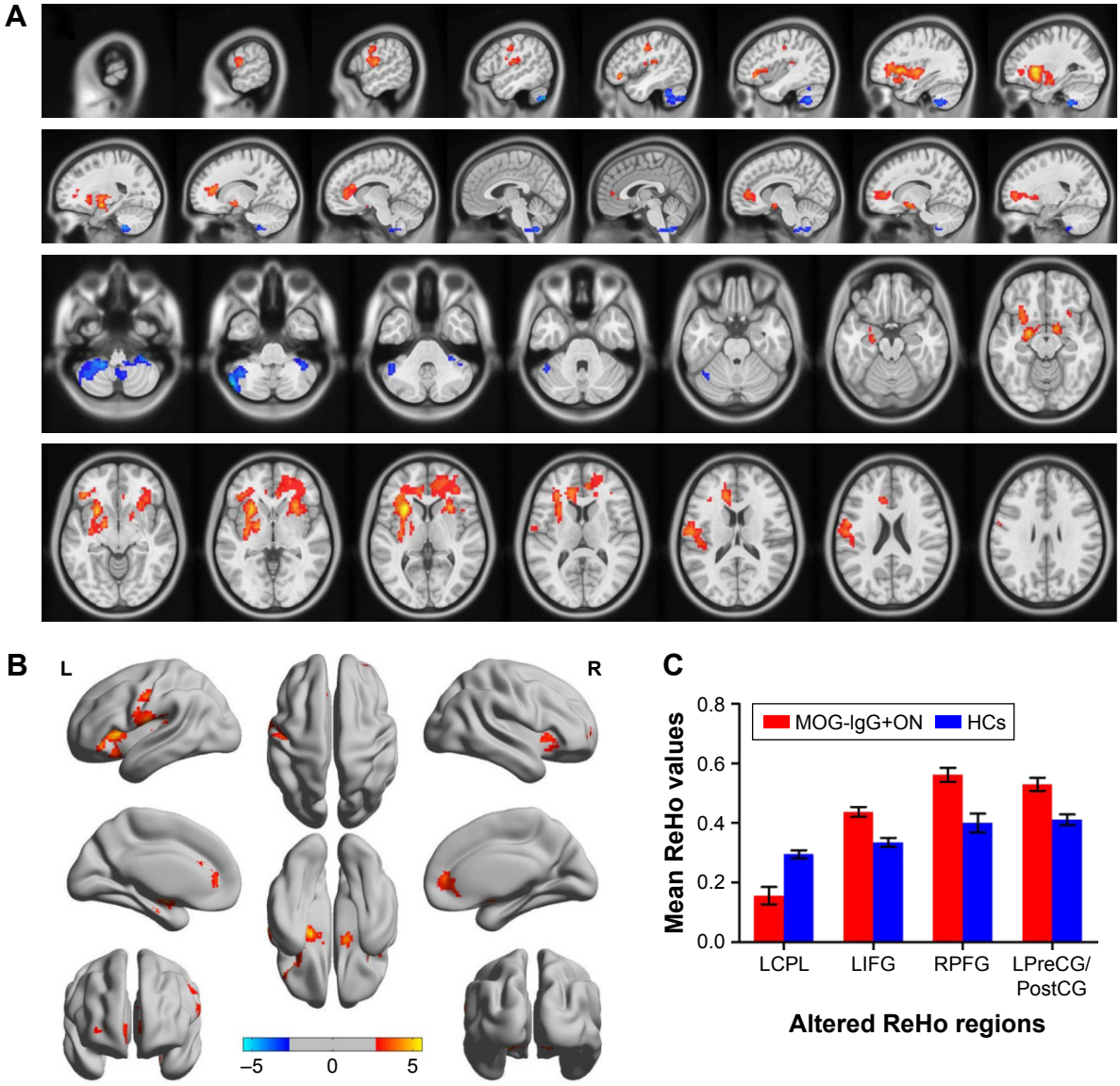

Figure 4 Spontaneous brain activity in the MOG-IgG+ON and HCs groups.
Notes: Significant activity differences were observed in the LCPL, LIFG, RPFG and LPreCG/PostCG. The red or yellow denotes higher ReHo values, and the blue areas indicate lower ReHo values ($P<0.01$ for multiple comparisons using GRF theory ($z>2.3$, $P<0.01$, cluster >40 voxels, AlphaSim corrected) (**A** and **B**). The mean values of altered ReHo values between the MOG-IgG+ON and HCs groups (**C**).
Abbreviations: GRF, Gaussian random field; HCs, healthy controls; L, left; LCPL, left cerebellum posterior lobe; LIFG, left inferior frontal gyrus; LPreCG/PostCG, left precentral/postcentral gyrus; MOG, myelin oligodendrocyte glycoprotein; NMO, neuromyelitis optica; ON, optic neuritis; R, right; ReHo, regional homogeneity; RPFG, right prefrontal gyrus.

Analysis of different ReHo values of AQP4-IgG+NMO-ON subjects and HCs

The MT visual area, known as the visual cortex 5, is located in the region of the extrastriate visual cortex. The MT plays a critical role in processing visual motion[33,34] and is involved in eye movements.[35] Liang et al[28] demonstrated that NMO patients have "deceased" ReHo values in the right MT gyrus. In addition, Wang et al[36] reported that NMO is associated with markedly decreased GM volume in the temporal cortices. Given these findings, we found that the AQP4-IgG+NMO-ON subjects had decreased ReHo values in the right MT gyrus, which indicated the dysfunction of these loci. Thus, we speculated that the AQP4-IgG+NMO-ON subjects might have impairment of the visual motion control on the basis of dysfunction in these temporal lobe zones.

The occipital lobe contains the visual cortex and plays an important role in visual processing. The visual cortex mainly includes visual areas V1, V2, V3, V4, and V5. There are two primary visual pathways comprising a ventral stream and a dorsal stream.[37] Pichiecchio et al[38] demonstrated that

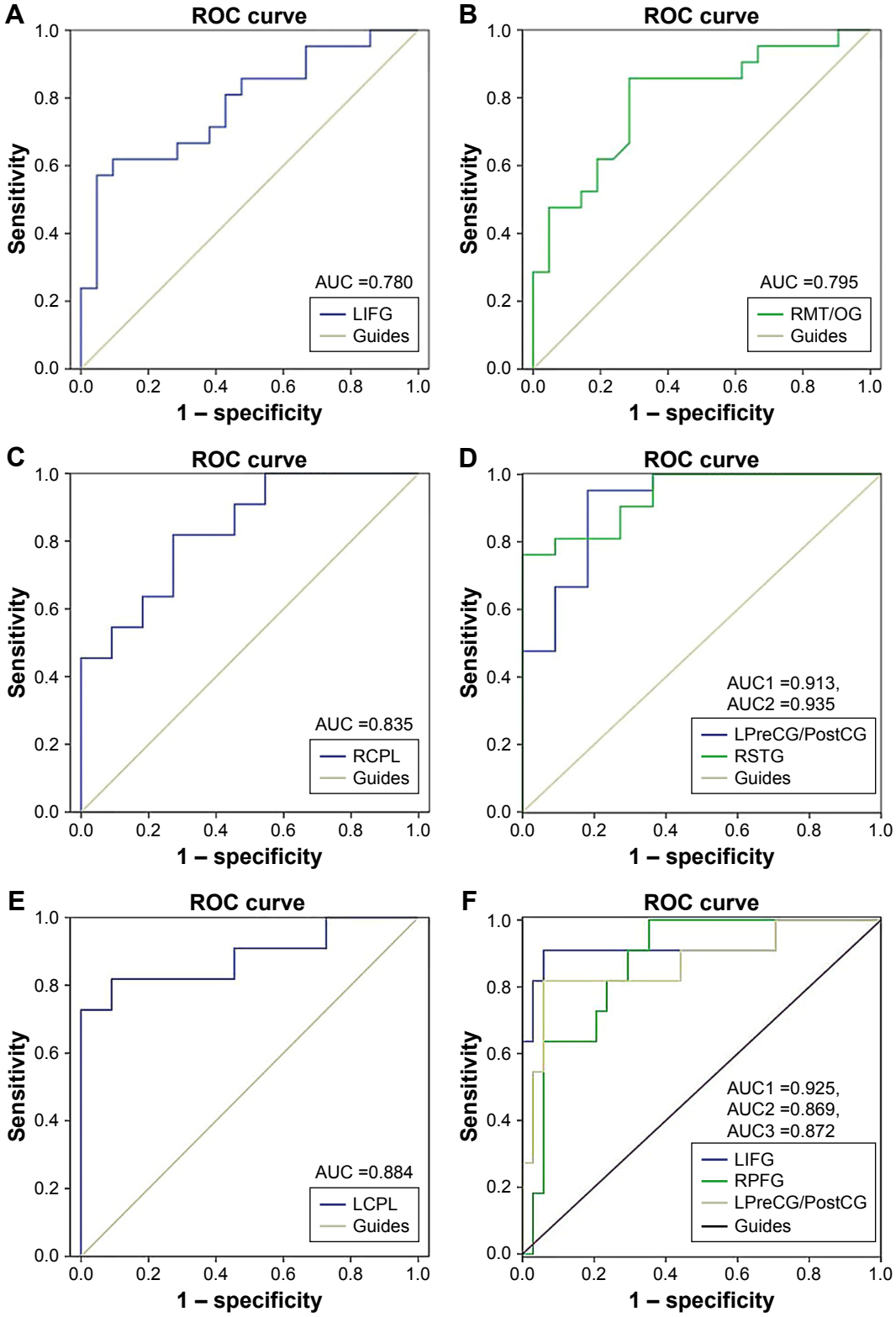

Figure 5 ROC curve analysis of the mean ReHo values for altered brain regions.

Notes: (**A**) ROC curve: AQP4-IgG+NMO-ON > HCs, for LIFG 0.780 (P=0.002; 95% CI: 0.639–0.921); (**B**) ROC curve: AQP4-IgG+NMO-ON < HCs, for RMT/OG 0.795 (P<0.001; 95% CI: 0.658–0.932); (**C**) ROC curve: AQP4-IgG+NMO-ON > MOG-IgG+ON, for RCPL 0.835 (P=0.008; 95% CI: 0.669–1.000); (**D**) ROC curve: AQP4-IgG+NMO-ON < MOG-IgG+ON, for LPreCG/PostCG 0.913 (P<0.001; 95% CI: 0.669–1.000) and RSTG 0.935 (P<0.001; 95% CI: 0.669–1.000); (**E**) ROC curve: MOG-IgG+ON < HCs, for LCPL 0.884 (P=0.002; 95% CI: 0.733–1.000); (**F**) ROC curve: MOG-IgG+ON > HCs, for LIFG 0.925 (P<0.001; 95% CI: 0.803–1.000), RPFG 0.869 (P<0.001; 95% CI: 0.763–0.975), and LPreCG/PostCG 0.872 (P<0.001; 95% CI: 0.732–1.000).

Abbreviations: AUC, area under the curve; AQP4, aquaporin-4; HCs, healthy controls; LCPL, left cerebellum posterior lobe; LIFG, left inferior frontal gyrus; LPreCG/PostCG, left precentral/postcentral gyrus; MOG, myelin oligodendrocyte glycoprotein; NMO, neuromyelitis optica; ON, optic neuritis; RCPL, right cerebellum posterior lobe; ReHo, regional homogeneity; RMT/OG, right middle temporal/occipital gyrus; ROC, receiver operating characteristic; RPFG, right prefrontal gyrus; RSTG, right superior temporal gyrus.

NMO patients have significantly decreased GM in the visual cortex. Meanwhile, Ringelstein et al[39] reported that there are reduced amplitudes and prolonged latencies in VEPs recorded in the eyes of AQP4-IgG+NMO patients. In support of these findings, in our study, the AQP4-IgG+NMO-ON group showed lower ReHo values in the right occipital gyrus, which reflected dysfunction in the occipital gyrus. Therefore, our results suggest that AQP4-IgG+NMO-ON subjects have impairment of the visual cortex.

The IFG is the part of the frontal gyrus that is involved in phonologic and semantic operations.[40] The IFG played a critical role in cognitive control.[41,42] In our study, we found that AQP4-IgG+ON subjects showed higher ReHo values in the left IFG, indicating the hyperfunction of the IFG. We speculated that AQP4-IgG+ON patients might be associated with dysfunction of cognitive control.

Analysis of different ReHo values between MOG-IgG+ON subjects and HCs

The posterior lobe of the CPL is located below the primary fissure. The cerebellum plays a critical role in motor control[43] and is involved in motor learning[44] and ocular motor control.[45] Recent research demonstrated that the cerebellum is closely related to cognition.[46,47] Rocca et al[48] found that the Devic's NMO was associated with increased activation in the sensorimotor network, including the cerebellum. Our study also demonstrated that MOG-IgG+ON subjects showed decreased ReHo values in the left CPL; this might suggest the dysfunction of the left CPL. Thus, we speculated that in MOG-IgG+ON subjects, this might lead to the impairment of motor control.

As with the AQP4-IgG+NMO-ON subjects, we also found that the MOG-IgG+ON subjects had increased ReHo values in the left IFG. We speculated that MOG-IgG+ON subjects might have dysfunction of cognitive control.

The prefrontal gyrus comprises the anterior part of the frontal lobe and is involved in executive functions,[49] spatial attention,[50] and emotion and cognition.[51,52] Previous studies demonstrated that NMO patients have impaired cognition.[53,54] Chanson et al[55] found that NMO patients had regions of atrophy of GM in the prefrontal cortex. Consistent with these findings, we found that our MOG-IgG+ON subjects had increased ReHo values in the right prefrontal gyrus, which indicated hyperactivity. Therefore, we speculated that MOG-IgG+ON subjects might have dysfunction of cognition and emotion.

The precentral gyrus is located on the surface of the posterior frontal lobe and is the site of the primary motor cortex. The precentral gyrus plays an important role in movement[56] quantity and frequency.[57] The postcentral gyrus is the location of the primary somatosensory cortex, which is involved in information processing of tactile stimuli.[58] The primary somatosensory cortex plays a critical role in pain perception.[59] Duan et al[60] found that NMO patients have lower WM volumes in the right precentral and postcentral gyri. Furthermore, NMO patients had impairment of their sensorimotor systems.[61] In our study, we demonstrated that MOG-IgG+ON subjects showed increased ReHo values in the left precentral/postcentral gyrus. Our result suggested that MOG-IgG+ON subjects might end up with impairment of the sensorimotor dysfunction.

Analysis of different ReHo values in AQP4-IgG+NMO-ON and MOG-IgG+ON subjects

In our study, the AQP4-IgG+NMO-ON group showed lower ReHo values in the left precentral/postcentral gyrus and right superior temporal gyrus and higher ReHo values in the right CPL compared with the MOG-IgG+ON group. The superior temporal gyrus was involved in auditory processing.[62,63] We speculated that the AQP4-IgG+NMO-ON group showed lesser synchronized neuronal activity in the sensory motor and auditory cortex than the MOG-IgG+ON group. Moreover, MOG-IgG+ON subjects had more synchronized neuronal activity in the motor control areas than AQP4-IgG+NMO-ON subjects.

Conclusion

Our results demonstrated that AQP4-IgG+NMO-ON and MOG-IgG+ON subjects showed abnormal synchronization of their neuronal activity in many brain regions, consistent with deficits in the visual, motor, and cognitive function. Furthermore, we also found altered synchronization of neuronal activity in the AQP4-IgG+NMO-ON and MOG-IgG+ON groups. ReHo values might prove to be a useful clinical indicator of dysfunctional brain activity in NMO subjects.

Acknowledgments

The authors thank the following authors who collected the fMRI data of the study: Mingge Li, Huanfen Zhou, Honglu Song, Da Teng, Dahe Lin, and Nanping Ai. This was not an industry-supported study. This work was supported by a grant from the National High Technology Research and Development Program of China (863 Program; No 2015AAO20511).

Disclosure

The authors report no conflicts of interest in this work.

References

1. Etemadifar M, Nasr Z, Khalili B, Taherioun M, Vosoughi R. Epidemiology of neuromyelitis optica in the world: a systematic review and meta-analysis. *Mult Scler Int*. 2015;2015:174720.
2. Lu Z, Qiu W, Zou Y, et al. Characteristic linear lesions and longitudinally extensive spinal cord lesions in Chinese patients with neuromyelitis optica. *J Neurol Sci*. 2010;293(1–2):92–96.
3. Siuko M, Tienari PJ, Saastamoinen KP, et al. Neuromyelitis optica and aquaporin-4 (AQP4) autoantibodies in consecutive optic neuritis patients in Southern Finland. *Acta Ophthalmol*. 2014;92(4):387–391.
4. Pisani F, Sparaneo A, Tortorella C, et al. Aquaporin-4 autoantibodies in neuromyelitis optica: AQP4 isoform-dependent sensitivity and specificity. *PLoS One*. 2013;8(11):e79185.
5. Luppe S, Robertson NP. MOG-IgG in neuromyelitis optica. *J Neurol*. 2014;261(3):640–642.
6. van Pelt ED, Wong YY, Ketelslegers IA, Hamann D, Hintzen RQ. Neuromyelitis optica spectrum disorders: comparison of clinical and magnetic resonance imaging characteristics of AQP4-IgG versus MOG-IgG seropositive cases in the Netherlands. *Eur J Neurol*. 2016; 23(3):580–587.
7. Stiebel-Kalish H, Lotan I, Brody J, et al. Retinal nerve fiber layer may be better preserved in MOG-IgG versus AQP4-IgG optic neuritis: a cohort study. *PLoS One*. 2017;12(1):e0170847.
8. Tanaka M, Kinoshita M, Tanaka K. Corticosteroid and tacrolimus treatment in neuromyelitis optica related disorders. *Mult Scler*. 2015; 21(5):669.
9. Abboud H, Petrak A, Mealy M, Sasidharan S, Siddique L, Levy M. Treatment of acute relapses in neuromyelitis optica: steroids alone versus steroids plus plasma exchange. *Mult Scler*. 2016;22(2):185–192.
10. Chen H, Qiu W, Zhang Q, et al. Comparisons of the efficacy and tolerability of mycophenolate mofetil and azathioprine as treatments for neuromyelitis optica and neuromyelitis optica spectrum disorder. *Eur J Neurol*. 2017;24(1):219–226.
11. Damato V, Evoli A, Iorio R. Efficacy and safety of rituximab therapy in neuromyelitis optica spectrum disorders: a systematic review and meta-analysis. *JAMA Neurol*. 2016;73(11):1342–1348.
12. Fan M, Fu Y, Su L, et al. Comparison of brain and spinal cord magnetic resonance imaging features in neuromyelitis optica spectrum disorders patients with or without aquaporin-4 antibody. *Mult Scler Relat Disord*. 2017;13:58–66.
13. Juryńczyk M, Tackley G, Kong Y, et al. Brain lesion distribution criteria distinguish MS from AQP4-antibody NMOSD and MOG-antibody disease. *J Neurol Neurosurg Psychiatry*. 2017;88(2):132–136.
14. Liu Y, Wang J, Daams M, et al. Differential patterns of spinal cord and brain atrophy in NMO and MS. *Neurology*. 2015;84(14):1465–1472.
15. Liu Y, Fu Y, Schoonheim MM, et al. Structural MRI substrates of cognitive impairment in neuromyelitis optica. *Neurology*. 2015;85(17): 1491–1499.
16. Rivero RL, Oliveira EM, Bichuetti DB, Gabbai AA, Nogueira RG, Abdala N. Diffusion tensor imaging of the cervical spinal cord of patients with neuromyelitis optica. *Magn Reson Imaging*. 2014;32(5): 457–463.
17. von Glehn F, Jarius S, Cavalcanti Lira RP, et al. Structural brain abnormalities are related to retinal nerve fiber layer thinning and disease duration in neuromyelitis optica spectrum disorders. *Mult Scler*. 2014;20(9): 1189–1197.
18. Cai H, Zhu J, Zhang N, et al. Subregional structural and connectivity damage in the visual cortex in neuromyelitis optica. *Sci Rep*. 2017;7: 41914.
19. Sturm AK, König P. Mechanisms to synchronize neuronal activity. *Biol Cybern*. 2001;84(3):153–172.
20. Bayati M, Valizadeh A, Abbassian A, Cheng S. Self-organization of synchronous activity propagation in neuronal networks driven by local excitation. *Front Comput Neurosci*. 2015;9:69.
21. Melloni L, Molina C, Pena M, Torres D, Singer W, Rodriguez E. Synchronization of neural activity across cortical areas correlates with conscious perception. *J Neurosci*. 2007;27(11):2858–2865.
22. Fukai T. Synchronization of neural activity is a promising mechanism of memory information processing in networks of columns. *Biol Cybern*. 1994;71(3):215–226.
23. Zang Y, Jiang T, Lu Y, He Y, Tian L. Regional homogeneity approach to fMRI data analysis. *Neuroimage*. 2004;22(1):394–400.
24. Tononi G, McIntosh AR, Russell DP, Edelman GM. Functional clustering: identifying strongly interactive brain regions in neuroimaging data. *Neuroimage*. 1998;7(2):133–149.
25. Zhang X, Tang Y, Zhu Y, Li Y, Tong S. Study of functional brain homogeneity in female patients with major depressive disorder. *Conf Proc IEEE Eng Med Biol Soc*. 2016;2016:2562–2565.
26. Dai XJ, Gong HH, Wang YX, et al. Gender differences in brain regional homogeneity of healthy subjects after normal sleep and after sleep deprivation: a resting-state fMRI study. *Sleep Med*. 2012;13(6): 720–727.
27. Zhang Z, Liu Y, Jiang T, et al. Altered spontaneous activity in Alzheimer's disease and mild cognitive impairment revealed by regional homogeneity. *Neuroimage*. 2012;59(2):1429–1440.
28. Liang P, Liu Y, Jia X, et al. Regional homogeneity changes in patients with neuromyelitis optica revealed by resting-state functional MRI. *Clin Neurophysiol*. 2011;122(1):121–127.
29. Wingerchuk DM, Lennon VA, Pittock SJ, Lucchinetti CF, Weinshenker BG. Revised diagnostic criteria for neuromyelitis optica. *Neurology*. 2006;66(10):1485–1489.
30. Shao Y, Cai FQ, Zhong YL, et al. Altered intrinsic regional spontaneous brain activity in patients with optic neuritis: a resting-state functional magnetic resonance imaging study. *Neuropsychiatr Dis Treat*. 2015;11:3065–3073.
31. Chao-Gan Y, Yu-Feng Z. DPARSF: a MATLAB toolbox for "Pipeline" data analysis of resting-state fMRI. *Front Syst Neurosci*. 2010; 14(4):13.
32. Lowe MJ, Mock BJ, Sorenson JA. Functional connectivity in single and multislice echoplanar imaging using resting-state fluctuations. *Neuroimage*. 1998;7(2):119–132.
33. Riecanský I. Extrastriate area V5 (MT) and its role in the processing of visual motion. *Cesk Fysiol*. 2004;53(1):17–22.
34. Ajina S, Kennard C, Rees G, Bridge H. Motion area V5/MT+ response to global motion in the absence of V1 resembles early visual cortex. *Brain*. 2015;138(pt 1):164–178.
35. Galletti C, Fattori P. Neuronal mechanisms for detection of motion in the field of view. *Neuropsychologia*. 2003;41(13):1717–1727.
36. Wang Q, Zhang N, Qin W, et al. Gray matter volume reduction is associated with cognitive impairment in neuromyelitis optica. *AJNR Am J Neuroradiol*. 2015;36(10):1822–1829.
37. Dixon P. Computation in the dorsal and ventral stream. *Cogn Neurosci*. 2010;1(1):63–64.
38. Pichiecchio A, Tavazzi E, Poloni G, et al. Advanced magnetic resonance imaging of neuromyelitis optica: a multiparametric approach. *Mult Scler*. 2012;18(6):817–824.
39. Ringelstein M, Kleiter I, Ayzenberg I, et al. Visual evoked potentials in neuromyelitis optica and its spectrum disorders. *Mult Scler*. 2014; 20(5):617–620.
40. Costafreda SG, Fu CH, Lee L, Everitt B, Brammer MJ, David AS. A systematic review and quantitative appraisal of fMRI studies of verbal fluency: role of the left inferior frontal gyrus. *Hum Brain Mapp*. 2006; 27(10):799–810.
41. Tops M, Boksem MA. A potential role of the inferior frontal gyrus and anterior insula in cognitive control, brain rhythms, and event-related potentials. *Front Psychol*. 2011;2:330.

42. Sundermann B, Pfleiderer B. Functional connectivity profile of the human inferior frontal junction: involvement in a cognitive control network. *BMC Neurosci*. 2012;13:119.
43. Paulin MG. The role of the cerebellum in motor control and perception. *Brain Behav Evol*. 1993;41(1):39–50.
44. Wada N, Funabiki K, Nakanishi S. Role of granule-cell transmission in memory trace of cerebellum-dependent optokinetic motor learning. *Proc Natl Acad Sci U S A*. 2014;111(14):5373–5378.
45. Kheradmand A, Zee DS. Cerebellum and ocular motor control. *Front Neurol*. 2011;2:53.
46. Koziol LF, Budding D, Andreasen N, et al. Consensus paper: the cerebellum's role in movement and cognition. *Cerebellum*. 2014;13(1):151–177.
47. Van Overwalle F, Mariën P. Functional connectivity between the cerebrum and cerebellum in social cognition: a multi-study analysis. *Neuroimage*. 2016;124(pt A):248–255.
48. Rocca MA, Agosta F, Mezzapesa DM, et al. A functional MRI study of movement-associated cortical changes in patients with Devic's neuromyelitis optica. *Neuroimage*. 2004;21(3):1061–1068.
49. Yuan P, Raz N. Prefrontal cortex and executive functions in healthy adults: a meta-analysis of structural neuroimaging studies. *Neurosci Biobehav Rev*. 2014;42:180–192.
50. Small DM, Gitelman DR, Gregory MD, Nobre AC, Parrish TB, Mesulam MM. The posterior cingulate and medial prefrontal cortex mediate the anticipatory allocation of spatial attention. *Neuroimage*. 2003;18(3):633–641.
51. Gray JR, Braver TS, Raichle ME. Integration of emotion and cognition in the lateral prefrontal cortex. *Proc Natl Acad Sci U S A*. 2002;99(6):4115–4120.
52. Kompus K, Hugdahl K, Ohman A, Marklund P, Nyberg L. Distinct control networks for cognition and emotion in the prefrontal cortex. *Neurosci Lett*. 2009;467(2):76–80.
53. He D, Wu Q, Chen X, Zhao D, Gong Q, Zhou H. Cognitive impairment and whole brain diffusion in patients with neuromyelitis optica after acute relapse. *Brain Cogn*. 2011;77(1):80–88.
54. Cardona JF, Sinay V, Amoruso L, Hesse E, Manes F, Ibáñez A. The impact of neuromyelitis optica on the recognition of emotional facial expressions: a preliminary report. *Soc Neurosci*. 2014;9(6):633–638.
55. Chanson JB, Lamy J, Rousseau F, et al. White matter volume is decreased in the brain of patients with neuromyelitis optica. *Eur J Neurol*. 2013;20(2):361–367.
56. Guigon E, Baraduc P, Desmurget M. Coding of movement- and force-related information in primate primary motor cortex: a computational approach. *Eur J Neurosci*. 2007;26(1):250–260.
57. Kim JA, Eliassen JC, Sanes JN. Movement quantity and frequency coding in human motor areas. *J Neurophysiol*. 2005;94(4):2504–2511.
58. Guic E, Carrasco X, Rodríguez E, Robles I, Merzenich MM. Plasticity in primary somatosensory cortex resulting from environmentally enriched stimulation and sensory discrimination training. *Biol Res*. 2008;41(4):425–437.
59. Kim W, Kim SK, Nabekura J. Functional and structural plasticity in the primary somatosensory cortex associated with chronic pain. *J Neurochem*. 2017;141(4):499–506.
60. Duan Y, Liu Y, Liang P, et al. White matter atrophy in brain of neuromyelitis optica: a voxel-based morphometry study. *Acta Radiol*. 2014;55(5):589–593.
61. Liu Y, Duan Y, He Y, et al. Altered topological organization of white matter structural networks in patients with neuromyelitis optica. *PLoS One*. 2012;7(11):e48846.
62. Reale RA, Calvert GA, Thesen T, et al. Auditory-visual processing represented in the human superior temporal gyrus. *Neuroscience*. 2007;145(1):162–184.
63. Domínguez-Borràs J, Trautmann SA, Erhard P, Fehr T, Herrmann M, Escera C. Emotional context enhances auditory novelty processing in superior temporalgyrus. *Cereb Cortex*. 2009;19(7):1521–1529.